JOURNAL OF GEOPHYSICAL RESEARCH, VOL. 114, A01101, doi:10.1029/2008JA013499, 2009

A practical database method for predicting arrivals of "average" interplanetary shocks at Earth

X. S. Feng,[1] Y. Zhang,[1,2] W. Sun,[3] M. Dryer,[4,5] C. D. Fry,[4] and C. S. Deehr[3]

Received 15 June 2008; revised 20 October 2008; accepted 7 November 2008; published 6 January 2009.

[1] A practical database method for predicting the interplanetary shock arrival time at L1 point is presented here. First, a shock transit time database (hereinafter called Database-I) based on HAFv.1 (version 1 of the Hakamada-Akasofu-Fry model) is preliminarily established with hypothetical solar events. Then, on the basis of the prediction test results of 130 observed solar events during the period from February 1997 to August 2002, Database-I is modified to create a practical database method, named Database-II, organized on a multidimensional grid of source location, initial coronal shock speed, and the year of occurrence of the hypothetical solar event. The arrival time at L1 for any given solar event occurring in the 23rd solar cycle can be predicted by looking up in the grid of Database-II according to source location, the initial coronal shock speed, and the year of occurrence in cycle 23. Within the hit window of ±12 h, the success rate of the Database-II method for 130 solar events is 44%. This could be practically equivalent to the shock time of arrival (STOA) model, the interplanetary shock propagation model (ISPM), and the HAFv.2 model. To explore the capability of this method, it is tested on new data sets. These tests give reasonable results. In particular, this method's performance for a set of events in other cycles is as good as that of the STOA and ISPM models. This gives us confidence in its application to other cycles. From the viewpoint of long-term periodicity for solar activity, it is expected that the Database-II method can be applicable to the next solar cycle 24.

Citation: Feng, X. S., Y. Zhang, W. Sun, M. Dryer, C. D. Fry, and C. S. Deehr (2009), A practical database method for predicting arrivals of ''average'' interplanetary shocks at Earth, *J. Geophys. Res.*, *114*, A01101, doi:10.1029/2008JA013499.

1. Introduction

[2] It has been well known for many years that transient events may lead to nonrecurrent disturbances of geomagnetic field. These geomagnetic activities, such as geomagnetic storms, are known to be well associated with interplanetary (IP) shocks. Some models have been developed on the basis of associations between features of solar activity and IP shocks. Three physics-based models are currently available for real-time prediction for the arrival of IP shocks at Earth using available solar data as input parameter, and they utilize empirical equations based on observation, simple models, and numerical simulations. These models are the shock time of arrival (STOA) model, the interplanetary shock propagation model (ISPM), and the Hakamada-Akasofu-Fry (HAF) model. The forecasting skills of the three models have been evaluated, and the statistical comparisons between them revealed that the performances of these three models were practically identical in forecasting the shock arrival time [*Smith et al.*, 2000, 2004; *Fry et al.*, 2003; *McKenna-Lawlor et al.*, 2006].

[3] Recently, some other methods have also been developed to predict the arrival time of a solar disturbance at Earth. *Manoharan et al.* [2004] provided an empirical method to predict the IP shock transit time to 1 AU on the basis of the CME initial speed. *Schwenn et al.* [2005] presented a prediction function of the shock's arrival time at Earth that used the lateral expansion speed of the CME. Combining the analytical study for the propagation of the blast wave from a point source in a moving, steady state, medium with variable density with the energy estimation method in the ISPM model, *Feng and Zhao* [2006] developed a new physics-based prediction method for the arrival time of IP shocks at Earth.

[4] A database method for predicting arrivals of IP shocks at Earth is presented in this paper. The database method is set up through two steps. First, on the basis of HAFv.1 code [*Fry*, 1985], hypothetical solar eruptive events (such as source location, initial coronal shock speed, and the year of occurrence within a solar cycle of the event) distributed on the solar surface and the whole 23rd solar cycle are used as samples to obtain their corresponding arrival times, which are components of Database-I. Then, shock transit time prediction

[1]Solar-Interplanetary-Geomagnetic Weather Group, State Key Laboratory of Space Weather, Center for Space Science and Applied Research, Chinese Academy of Sciences, Beijing, China.
[2]School of Earth Sciences, Graduate University of the Chinese Academy of Sciences, Beijing, China.
[3]Geophysical Institute, University of Alaska, Fairbanks, Alaska, USA.
[4]Exploration Physics International, Inc., Huntsville, Alabama, USA.
[5]Space Weather Prediction Center, National Oceanic and Atmospheric Administration, Boulder, Colorado, USA.

0148-0227/09/2008JA013499$09.00

Database-II is created through a modification of Database-I made by considering initial shock speed and source longitude's impact on transit time. With Database-II, given the input parameters (source location, initial shock speed, and the year of occurrence of the observed solar events), then the shock arrival time may be obtained. The statistical comparisons between the arrival times obtained from Database-II and the observations will be also discussed in this paper.

[5] In the present paper, three forecasting models are introduced briefly in section 2. In section 3, we describe the construction of shock transit time Database-I. Section 4 provides the creation of Database-II through the prediction test and modification of Database-I. The comparisons of Database-II prediction results between our method and the STOA, ISPM, and HAFv.2 models are presented in section 5. Summary and conclusions are in section 6.

2. Operational Forecasting Models

[6] In this section, we briefly describe the three operational arrival time models: STOA, ISPM, and HAFv.2.

2.1. STOA Model

[7] The STOA model is based on similarity theory of blast waves, modified by the piston-driven concept, that emanate from point explosions [*Dryer and Smart*, 1984; *Smart et al.*, 1984, 1986; *Smart and Shea*, 1985; *Lewis and Dryer*, 1987]. The model assumes that an interplanetary shock propagates explosively, much like a supernova explosion, and predicts the shock arrival time at the Earth using the velocity of the disturbance within the corona determined from observation of type II solar radio bursts at metric wavelengths. In this model, the shock decelerates to a blast wave as it expands outward with $V_s \propto R^N$ (where $N = -(1/2)$, and R is the heliocentric radial distance). The magnitude of the total energy conversion process determines the solid angle of quasi-spherical shock propagation and how far it would propagate as it "rides over" a uniform background solar wind. It is assumed that the fastest part of the shock is nearly coincident with the heliocentric radius vector from the center of the Sun through the flare site. The shock speed directly above the flare is calculated from the type II radio frequency drift rate based on an assumed coronal density model. STOA uses a cosine function to account for the longitudinal dependence of the shock geometry in the ecliptic plane. The shock speed is assumed to decrease from the maximum in the direction of the flare via this cosine function, to give a nonspherical shape in longitude. This spatially dependent shock speed is taken to be constant during the piston driven phase. During the blast wave phase, the longitudinal cosine shape is maintained. STOA allows for a radial-varying background solar wind, which is uniform in solar longitude. This is estimated from the solar wind velocity V_{sw} measured at L1 at the time of the flare. Required observational data are as follows: V_s (discussed above), the flare's solar longitude; start time of the metric type II radio drift (essentially the peak time of the soft X-ray flux); the proxy piston-driving time duration; and the background solar wind velocity, V_{sw}.

[8] Noting observational and numerical findings that the radial dependence of shock wave velocity depends on initial shock wave velocity, *Moon et al.* [2002] suggest a simple modified STOA model (STOA-2) which has a linear relationship between initial coronal shock wave velocity (V_s) and its deceleration exponent (N), $N = 0.05 + 4 \times 10^{-4} V_s$, where V_s is a numeric value expressed in units of km/s. *Moon et al.* [2002] show that the STOA-2 model not only removes a systematic dependence of the transit time difference predicted by the previous STOA model on initial shock velocity, but also reduces the number of events with large transit time differences.

2.2. ISPM Model

[9] The ISPM model is based on a parametric study of 2.5 D MHD simulations [*Smith and Dryer*, 1990]. In their study, the net energy input into the solar wind is the main organizing parameter. If the net energy ejected into the solar wind by a solar source and its longitude are known, then the transit time and strength of the shock to 1 AU may be computed from algebraic equations given in this model. *Smith and Dryer* [1995] give the details of this model and the functions in energy-longitude space. Since the energies of solar ejecta are not available from observations, a method is given to estimate the net input energy from proxy input data. The model has predicted arrival times using input parameters: the velocity of disturbance (based on observation of type II solar radio bursts), the duration of flare (observed by the GOES satellite), and the location of flare occurrence on the Sun. The ISPM also gives an estimate of the shock strength index (SSI) providing a threshold below which shocks decay to MHD waves and SSI is used as an indicator of confidence in the prediction.

2.3. HAFv.2 Model

[10] The HAF model is a "modified kinematic" model described by *Hakamada and Akasofu* [1982], *Fry* [1985], *Fry et al.* [2001, 2003], and *Sun et al.* [1985]: "kinematic" in that the model kinetically projects the flow of the solar wind from inhomogeneous sources near the Sun out into interplanetary space; and "modified" in that the model adjusts the flow for stream-stream interactions as faster streams overtake slower ones. It can predict solar wind conditions (speed, density, and interplanetary magnetic field) at the Earth on the basis of observations of the Sun. It is a useful tool for the study of large-scale solar wind structure, especially for the investigation of propagation of the disturbances in interplanetary space.

[11] The HAF model has two components: background solar wind and event-driven solar wind. The background solar wind is established by the inner boundary conditions. The inputs of background component to HAFv.2 model are as follows.

2.3.1. Coronal Magnetic Field

[12] The coronal magnetic field and the outflow of plasma establish the ambient solar wind structure. Observations by various solar observatories of line-of-sight photospheric magnetic fields are individually combined to construct daily, synoptic, magnetogram maps of the radial magnetic field. These maps provide the steady state magnetic field boundary conditions that drive the HAFv.2 model background solar wind.

2.3.2. Background Solar Wind Speed

[13] Velocity at the source surface at 2.5 R_s was computed using the Wang-Sheeley-Arge algorithm [*Wang and Sheeley*, 1990; *Wang et al.*, 1997; *Arge and Pizzo*, 2000]. Since divergence of the magnetic field flux tubes from the photosphere to the source surface is inversely related to the solar wind

speed observed at 1 AU [*Wang and Sheeley*, 1990; *Wang et al.*, 1997], this can be utilized to estimate the radial solar wind velocity at 2.5 R_s.

2.4. Inputs for Solar Events

[14] The disturbance source of all three models was represented by a velocity enhancement localized in time and space. The event location, peak speed, and temporal profile were based on coincident optical, radio, and X-ray observations. Other data, such as CMEs were considered when available in near real time.

2.4.1. Source Location

[15] To establish the locations of individual events in heliolatitude and heliolongitude in a Sun-centered coordinate system, solar flare observations made by global, ground- and space-based observatories and spacecraft were utilized for real-time operational reasons and published later by NOAA-NGDC in Solar Geophysical Data.

2.4.2. Initial Coronal Shock Speed and Start Time

[16] The coronal shock speeds (V_s), are normally derived from metric type II radio frequency drift rates (downward in frequency) as a function of time. The events start time is taken to be the start of the metric type II.

2.4.3. Shock Driving Time

[17] The temporal profile of the shock speed at the solar source is governed by a time constant τ, which is the difference between the risetime of the integrated X-ray flux (in the 1–8 Angstrom channel on GOES 7) and the time of its decrease, measured linearly on the logarithmic flux scale at a level set at half the distance from the background level to the peak. The plasma speed is ramped from the background to a maximum value of V_s (the type II drift speed or its equivalent), and then decays. For the HAF code, the rise and decay are exponential [*Hakamada and Akasofu*, 1982]. The other two models just use linear ramps, but the numbers of points are so few so that this is usually immaterial. After recalling the above three operational forecasting models for arrival time prediction, we turn attention to our establishment of the shock transit time database.

3. Establishment of Shock Transit Time Database-I

[18] In this section, we first define samples of hypothetical solar transient events, and then obtain the arrival time at Earth for each hypothetical solar transient event by using the HAFv.1 code. Database-I will be constructed from hypothetical solar transient events and their computed transit times.

3.1. Definition of a Hypothetical Solar Transient Event

3.1.1. Source Location of a Hypothetical Solar Transient Event

[19] In order to construct Database-I, the solar source surface was sliced into a grid of 5° by 5° cells. Figure 1 shows a fragment of the grid of solar source surface. The central point of a rectangular cell is denoted by (θ_i (heliolatitude); φ_j (heliolongitude)). For latitude, solar events are mainly distributed within ±40° of the solar equator [*Zhao et al.*, 2006], so we choose the domain of θ and φ: $-50° \le \theta \le 50°$ and $-180° \le \varphi \le 180°$ ($\varphi = 0°$ points to the Earth's position). Thus, we have 21 × 72 cells in $[-50°, 50°] \times [-180°, 180°]$. $[\theta_i, \varphi_j]$ will be the source location of a hypothetical solar event. Therefore, for any given solar transient event, its source location is matched to one of cells constructed above.

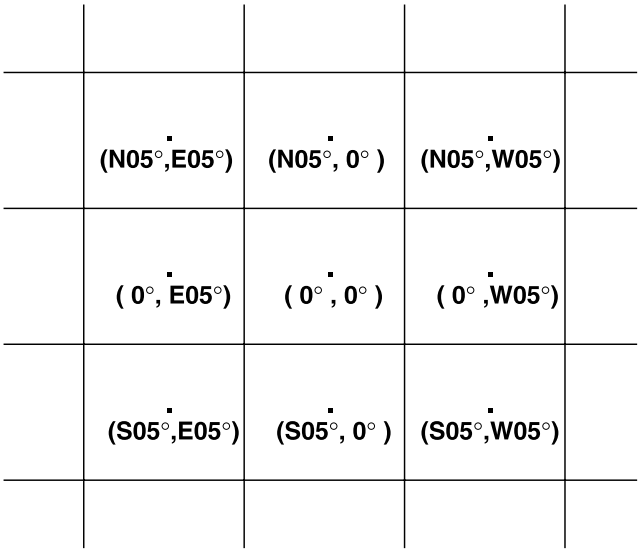

Figure 1. The fragment of the grid of solar source surface. The center point in a cell is the source location of a hypothetical solar event.

3.1.2. Initial Shock Speed of a Hypothetical Solar Transient Event

[20] The observed initial coronal shock speeds of a solar transient event usually range from 200 km/s to 2000 km/s. Thus, we use this range for the initial coronal shock speed of our hypothetical solar event at a fixed source location and we used 100 km/s for the grid size. That is, the initial shock speed V_{sk} of a hypothetical solar event at a fixed source location is an integer multiple of 100 km/s between 200 km/s and 2000 km/s; that is, $V_{sk} = 200 + 100 \times k$ (in km/s), with $k = 0, 1, \ldots, 18$.

3.1.3. Background Solar Wind of a Hypothetical Solar Transient Event

[21] The time range of Database-I covers all 11 years of solar cycle 23. In the HAFv.2 model, the solar source surface maps (magnetic field and solar wind velocity maps) can be updated daily. But in the construction of Database-I, for simplicity, we use the yearly variation of solar surface maps in an 11-year solar cycle. In order to obtain the background solar wind inputs to HAF code, we use the yearly mean magnetic field and yearly mean solar wind velocity maps on solar surface for each year of solar cycle 23. That is, the background solar wind is the same for all hypothetical solar transient events occurring in Y_n (the nth year in the 23rd solar cycle).

[22] Thus we define a hypothetical solar transient event by the parameters (θ_i, φ_j, V_{sk}, Y_n). Here, (θ_i, φ_j) is its source location, V_{sk} is its initial coronal shock speed, and Y_n is the year in which the solar transient event occurs, where $i = 0, \ldots, 20$; $j = 0, \ldots, 71$; $k = 0, \ldots, 18$; and $n = 0, \ldots, 10$. Therefore there are 21 × 72 × 19 × 11 hypothetical events distributed on the solar surface in Database-I for the whole 23rd cycle.

3.2. Shock Arrival Time of a Hypothetical Solar Transient Event

[23] In order to determine the shock transit time of a hypothetical solar transient event by using HAF code, we

need additional parameters: shock driving time and shock search index (SSI), in addition to the parameters mentioned in section 3.1.

3.2.1. Shock Driving Time

[24] The time profile of the shock speed at the solar source, which is an important input parameter of the HAF code, is governed by a time constant τ (called shock driving time). Of all of the input parameters required by the HAF code, the HAF code is least sensitive to τ. Therefore τ is determined from the empirically derived function $\tau = V_s/900$ h, where V_s is in km/s [*Howard et al.*, 2007].

3.2.2. Threshold of SSI

[25] In HAF model, the shock arrival time (SAT) is determined by computing predicted solar wind speed, density, and dynamic pressure at L1 spacecraft position for several days into the future. The predicted SATs are extracted from automatic scans of the temporal profiles of the dynamic pressure simulated at L1 using a SSI: $SSI = \log(\Delta P/P_{\min})$, where P is either the dynamic pressure or momentum flux; ΔP is the difference in P during consecutive 1-h time steps, and $P_{\min}$ is the minimum P value for these time steps. Shock arrival time was identified as the time of maximum SSI as long as SSI exceeds the threshold, which was found to be -0.35 in HAFv.2 model [*Fry et al.*, 2003]. For the Database-I method, the threshold of SSI is assumed to be -1.4, which will be validated below by the 380 events data taken from *Fry et al.* [2003] and *McKenna-Lawlor et al.* [2006] for the ascending and maximum phases, respectively, of cycle 23 as noted earlier. We will use testing sets below from these real-time studies in section 4. This value is different from that used by *Fry et al.* [2003]; a probable explanation for this difference is that we used the HAFv.1 code instead of HAFv.2 code. The improvements on the HAFv.1 model can be found in the work of *Fry et al.* [2001]. Therefore, by using the HAF code, SATs can be determined for all hypothetical events mentioned in section 3.1.

3.3. Shock Transit Time Database-I

[26] Database-I contains hypothetical solar transient events and their computed transit times. The parameters of Database-I are as follows: source location (θ_i, φ_j), initial shock speed (V_{sk}), the year of occurrence (Y_n), and the shock transit time (TT_{ijkn}), where $i = 0, \ldots, 20$; $j = 0, \ldots, 71$; $k = 0, \ldots, 18$; and $n = 0, \ldots, 10$.

[27] Suppose that an observed solar transient event is given with the source location (θ_o, φ_o), initial coronal shock speeds (V_{so}), which occurred in year (Y_o). Using Database-I, we can obtain the shock transit time for a given observed solar transient event by the following procedure.

[28] First, find Y_n by subtracting Y_o, the start of the solar cycle. Then, find the grid point (θ_i, φ_j) that is closest to that of the observed source location (θ_o, φ_o).

[29] Determine which V_{sk} in Database-I is closest to the initial coronal shock speed V_{so} of the observed solar transient event. Thus, from Database-I we can find the shock transit time TT_{ijkn} for the hypothetical solar transient event: (θ_i; φ_j; V_{sk}; Y_n). The hypothetical solar transient event with (θ_i; φ_j; V_{sk}; Y_n) can be seen approximately as a proxy of the given observed event with (θ_o; φ_o; V_{so}; Y_o), and the shock transit time (TT_{ijkn}) of the hypothetical solar transient event can be used as the shock transit time of the given observed one.

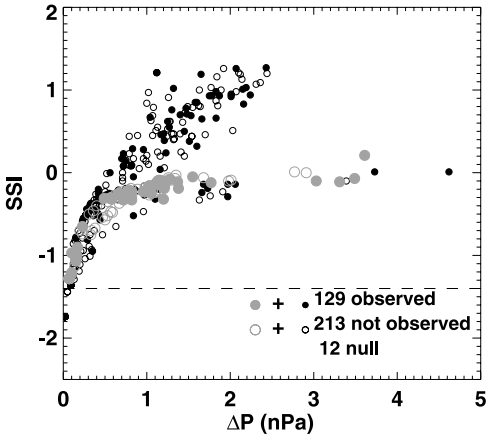

Figure 2. Shock search index (SSI) versus predicted difference in momentum flux across the shock (ΔP) for 129 predictions where shocks were observed (gray dots and smaller black dots) and 213 predictions where no shock was observed (gray circles and smaller black circles); 12 predictions were "correct nulls." The predictions occurring in 1997–1999 are indicated by gray dots and gray circles, while the predictions occurring in 2000–2002 are indicated by smaller black dots and smaller black circles.

[30] To see if our definition of SSI works, we employed the 380 events data during the periods from February 1997 to August 2002 as a testing set. The events with an ambiguous relationship between the solar event and the shock at 1 AU and those with initial shock speeds $V_s > 2000$ km/s are not included here. This leaves 354 events. Utilizing the procedure presented above, we determine SSI and ΔP for each observed solar event by finding the hypothetical events closest to it. Figure 2 shows SSI versus ΔP for the 342 events where the Database-I method predicted a shock arrival at Earth. Of the 354 events, 12 events were found not to result in significant disturbances at Earth (SSI < -1.4), and for the remaining 342 events, the associated disturbances were found to be shocks (SSI > -1.4). Among the 342 events with SSI > -1.4, there are 129 events where shocks were observed (Figure 2, gray dots and smaller black dots) and 213 events where no shock was observed (Figure 2, gray circles and smaller black circles). Note that all except one of the events with observed shocks lie above the line SSI $= -1.4$. Therefore our choice of the threshold for a shock prediction at SSI > -1.4 allows for the correct prediction of almost all observed shocks. It is interesting that a bifurcation can be seen in Figure 2. One branch is the predictions of 1997–1999 (rising phase) indicated by gray dots and gray circles in Figure 2; the other is the predictions of 2000–2002 (maximum phase) indicated by smaller black dots and smaller black circles in Figure 2. The ΔP value for a SSI value is higher in the rising phase than that in the maximum phase. This suggests that the shock would be more easily formed at 1 AU in the maximum phase than in the rising phase.

4. Establishment of Shock Transit Time Database-II

[31] In this section, we present our tentative results on the prediction of the arrival times using Database-I and then

Table 1. Event Input Parameters for the STOA, ISPM, and HAFv.2 Models and the Database-II Method[a]

Event	Begin Date	Begin Time (UT)	Source Location	V_s (km/s)	τ (h)	Flare Classification: X-ray/Optical	V_{sw} (km/s)
1	19970207	0230	S49°, W02°	600	6	XX	400
2	19970407	1358	S30°, E19°	800	0.5	3N	425
3	19970512	0516	N21°, W08°	1400	2.5	XX	300
4	19971104	0608	S14°, W33°	1400	1.25	2B	350
5	19971127	1317	N20°, E60°	700	0.34	2B	370
6	19980126	2214	N16°, E24°	900	0.5	XX	400
7	19980519	0953	N29°, E46°	1000	0.5	XX	420
8	19980611	1006	N20°, W00°	700	3	XX	400
9	19980808	0318	N30°, E09°	600	1	XX	400
10	19980824	2200	N30°, E09°	1300	2	3B	400
11	19980903	1417	S22°, E03°	700	2	XX	480
12	19980923	0656	N20°, E07°	1600	0.8	3B	470
13	19980930	1332	N23°, W81°	1200	1.68	2N	400
14	19981020	2320	N15°, W92°	1100	2	XX	500
15	19981105	1951	N18°, W21°	900	1.2	2B	400
16	19981128	0554	N20°, E33°	1000	3	3N	360
17	19981223	0659	N29°, E83°	850	3	XX	340
18	19990120	2004	N30°, E10°	800	4	XX	425
19	19990209	0519	S25°, W24°	600	1.5	SF	350
20	19990216	0257	S23°, W14°	900	1.75	SF	450
21	19990216	2126	N19°, W12°	700	0.1	1N	450
22	19990308	0638	S22°, E76°	700	0.75	SF	450
23	19990622	1824	N24°, E30°	1400	1	1N	320
24	19990629	0515	N18°, E07°	750	0.25	SF	500
25	19990711	0013	N13°, E32°	650	0.33	XX	280
26	19990719	0216	N12°, W16°	500	2.5	SF	320
27	19990725	1338	N38°, W81°	1000	3	SF	440
28	19990728	1820	S19°, E22°	500	3	1N	380
29	19990801	2110	N27°, E16°	700	1	SF	420
30	19990806	1641	S28°, W92°	900	1	SF	450
31	19990820	2317	S25°, E64°	700	0.5	1N	500
32	19990821	1652	S25°, E56°	500	0.25	1B	460
33	19990828	1807	S26°, W14°	600	2	2N	650
34	19990830	1803	N18°, W16°	700	2	SF	530
35	19990913	1622	N15°, W17°	500	1.25	SF	550
36	19991117	0959	N17°, E21°	900	0.5	2B	400
37	19991120	2239	S16°, E01°	700	1.5	2B	400
38	19991124	2333	S19°, W43°	550	1	SF	380
39	19991222	0201	N10°, E30°	500	1	2B	300
40	19991228	0056	N20°, W56°	702	0.33	2B	400
41	20000118	1719	S09°, E11°	400	1.5	1N	320
42	20000208	0857	N25°, E26°	600	2	1B	500
43	20000210	0148	N31°, E04°	1100	1.5	XX	440
44	20000212	0406	N26°, W23°	700	1	1N	550
45	20000218	0920	S16°, W78°	1400	1	SF	550
46	20000404	1525	N16°, W66°	2000	1	2F	400
47	20000420	2113	S23°, W45°	600	0.5	SF	550
48	20000430	0805	S11°, W18°	700	2	1N	400
49	20000510	1938	N14°, E20°	680	2.5	2N	340
50	20000512	2316	S23°, W31°	581	1	SF	400
51	20000520	0556	S15°, W08°	500	1	1N	450
52	20000606	1523	N20°, E13°	1189	1.5	XX	460
53	20000607	1550	N18°, E01°	826	1	3B	525
54	20000615	1946	N20°, W65°	996	1.25	2N	600
55	20000618	0158	N23°, W85°	660	0.25	SF	400
56	20000620	1932	N19°, W28°	980	0.33	1N	370
57	20000707	1114	N23°, W41°	800	2	SN	380
58	20000710	2123	N18°, E49°	1300	2.5	2B	450
59	20000712	2014	N17°, W65°	950	0.67	SF	480
60	20000714	1020	N22°, W07°	1800	1.5	3B	300
61	20000717	2021	S11°, E36°	600	0.25	1N	550
62	20000722	1125	N14°, W56°	1000	1.33	2N	410
63	20000725	0249	N06°, W03°	903	0.25	2B	360
64	20000901	1827	N10°, W60°	500	1	1N	400
65	20000912	1207	S17°, W09°	1030	4	2N	380
66	20001001	1312	S10°, E15°	1100	1.5	1F	400
67	20001009	2338	N01°, W14°	925	3	1F	350
68	20001029	0148	S25°, E35°	1200	1	2B	400
69	20001101	1610	S17°, E39°	700	1	C2.2/?	360
70	20001123	2326	N22°, W03°	1025	0.5	M1.0/1N	360
71	20001125	1844	N19°, W23°	916	3	X1.9/2B	400
72	20001126	0308	N19°, W38°	800	1	M2.2/1F	600

Table 1. (continued)

Event	Begin Date	Begin Time (UT)	Source Location	V_s (km/s)	τ (h)	Flare Classification: X-ray/Optical	V_{sw} (km/s)
73	20001126	1655	N18°, W38°	1000	0.83	X4.0/2B	600
74	20001129	0629	S13°, E43°	528	0.33	C9.1/SF	550
75	20001218	1111	N15°, E01°	700	0.25	C7.0/SF	350
76	20010110	0042	N13°, E36°	1200	1	C5/1N	360
77	20010120	2114	S07°, E46°	1300	1	M7.7/2B	315
78	20010128	1600	S04°, W59°	1000	1	M1.5/?	400
79	20010211	0104	N24°, W57°	670	1.5	C6.5/1F	400
80	20010215	1308	N18°, E20°	1000	3	B8.8/?	470
81	20010315	2159	N11°, W09°	500	3	C1.9/SF	320
82	20010318	0852	S05°, W27°	380	0.17	C3.1/SF	330
83	20010328	1240	N18°, E02°	1000	4	M4.3/SF	600
84	20010329	1004	N16°, W12°	1300	2	X1.7/1N	600
85	20010331	1132	N16°, W34°	1200	1	M2.1/SF	600
86	20010405	1725	S24°, E50°	1100	2.5	M5.1/2N	500
87	20010406	1921	S21°, E31°	2000	0.5	X5.6/SF	500
88	20010409	1527	S21°, W04°	800	2	M7.9/2B	560
89	20010411	1317	S22°, W27°	1231	1.5	M2.3/1F	700
90	20010426	1335	N20°, W04°	1000	3	M7.8/2B	430
91	20010524	1940	N07°, E29°	620	2	M1.2/1N	550
92	20010615	1007	S26°, E41°	970	1	M6.3/1N	360
93	20010730	2045	N05°, E76°	700	0.25	C6.0/?	400
94	20010814	1242	N26°, W10°	700	4	C2.3/SF	475
95	20010825	1632	S17°, E34°	1280	2	X5.3/3B	380
96	20010828	1603	N14°, E69°	1127	0.67	M1/SN	500
97	20010830	0147	N12°, E52°	800	0.33	C5/SF	400
98	20010830	2035	N15°, E44°	1500	0.17	M3.0/1N	400
99	20010909	1517	S17°, E03°	868	0.33	M3.4/1N	300
100	20010925	0440	S18°, W01°	450	0.25	M7.6/1N	250
101	20011009	1055	S23°, E17°	650	1.67	M1.4/2F	460
102	20011019	0101	N16°, W18°	914	1	X1.6/2B	330
103	20011025	1456	S19°, W20°	1091	1.5	X1.3/3B	450
104	20011104	1610	N02°, W23°	1329	1.75	X1.0/3B	320
105	20011108	0703	S19°, W19°	1000	0.17	M9.1/1N	500
106	20011117	0450	S13°, E42°	560	4	M2.8/1N	420
107	20011121	1324	S15°, W18°	700	5	C4.7/SF	370
108	20011122	2027	S25°, W67°	900	1	M3.8/2B	440
109	20011122	2231	S15°, W34°	1000	1.5	M9.9/2B	440
110	20011226	0502	N08°, W54°	1500	4	M7.1/1B	380
111	20011228	2005	S20°, E97°	1359	3.67	X3.4/?	360
112	20020103	0221	S11°, E12°	465	1	C6.0/1F	360
113	20020123	1341	N12°, E29°	562	0.5	C3.7/SF	380
114	20020127	1214	N18°, W63°	500	2	C3/SN	360
115	20020224	1453	S18°, W44°	802	0.67	C4.4/SF	325
116	20020312	2319	S22°, E93°	1000	0.67	M1.5/SF	460
117	20020315	2216	S08°, W03°	425	5	M2.1/1F	340
118	20020318	0231	S10°, W40°	1000	4.5	M1.0/?	470
119	20020414	0744	N19°, W57°	730	0.17	C9.6/SF	410
120	20020417	0808	S14°, W35°	814	4.5	?/SF	350
121	20020507	0353	S10°, E27°	1500	1	M1.4/?	400
122	20020516	0028	S22°, E14°	420	3	C4.5/?	400
123	20020517	0810	N07°, E90°	380	3	M1.5/?	380
124	20020521	2128	N17°, E38°	670	1.33	M1.5/2F	400
125	20020715	2008	N19°, W01°	1200	2	X3.0/3B	340
126	20020717	0706	N21°, W17°	1022	0.5	M8.5/1B	500
127	20020718	0747	N19°, W30°	998	0.25	X1.8/2B	500
128	20020723	0029	S13°, E72°	1600	1.25	X4.8/2B	500
129	20020726	2112	S19°, E26°	1200	4	M8.7/2N	440
130	20020729	0240	S21°, W12°	600	0.5	M4.8/1F	480

[a]These events are taken from the work of *Fry et al.* [2003] and *McKenna-Lawlor et al.* [2006]. The events without a corresponding IP shock arrival at 1 AU, those with an ambiguous relationship between the solar event and the shock at 1 AU, and those with $V_s > 2000$ km/s are not included here. The detailed input parameters for these events can be found in the work of *Fry et al.* [2003] and *McKenna-Lawlor et al.* [2006]. Begin time is given as year, month, day (YYMMDD) and as time in UT of the start of the metric type II radio burst. The source location is the location of the associated optical flare. V_s is the velocity of the shock in the coronal, estimated from the type II frequency drift. The τ is the duration of the solar event, estimated from the X-ray flux. Classifications of the associated X-ray and optical flares are given when available, and XX indicates that optical data are unavailable. V_{sw} is the speed of the solar wind at L1 at the time of the solar event. V_{sw} is listed only to give an indication of the 1 AU conditions at Earth at the time of the flare. Also, flare classifications are listed only for supplementary information.

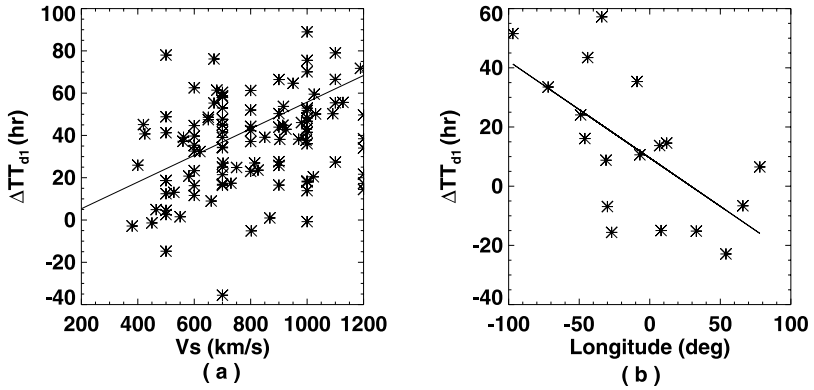

Figure 3. The error in the predicted transit time (ΔTT_{d1}) plotted versus (a) V_s for $V_s \leq 1200$ km/s and (b) heliographic longitude for $V_s > 1200$ km/s. The solid lines denote linear fittings.

provide its modification according to our test results and observations, which leads us to the establishment of shock transit time Database-II.

4.1. Prediction of the Database-I Method

[32] Comparisons between the predicted and observed shock arrival times have been made for a sample of 173 shock events recorded during the rising time of solar cycle 23 and 166 events recorded during the maximum of the same solar cycle, respectively [*Fry et al.*, 2003; *McKenna-Lawlor et al.*, 2006]. For testing purposes, we have collected 130 "average" shock events (solar flare IP shock events with speeds in the range 200 km/s $\sim$ 2000 km/s) that arrived at Earth during the period from February 1997 to August 2002 (listed in Table 1) from published papers [*Fry et al.*, 2003; *McKenna-Lawlor et al.*, 2006]. Moreover, the events without

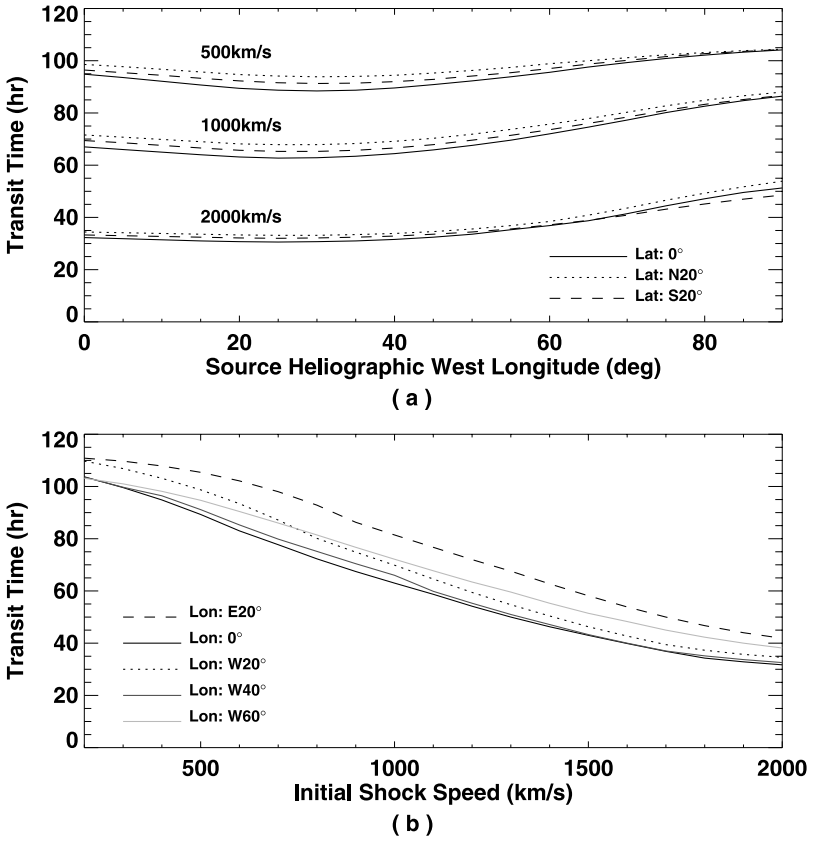

Figure 4. (a) Variation of shock transit time as a function of the sine of heliographic longitude of the source event for shocks with initial speeds of 500, 1000, and 2000 km/s. Curves for several values of heliographic latitude are shown by a dashed line for S20°, by a solid line for 0°, and a dotted line for N20°. (b) Variation of shock transit time for heliolongitude of E20° (dashed line), 0° (black solid line), W20° (dotted line), W40° (gray solid line), and W60° (light gray solid line).

Table 2. Observed and Predicted Shock Arrival Times for the Events in Table 1[a]

Event	SAT Date	SAT Time (UT)	TT_o (h)	TT_s (h)	TT_i (h)	TT_h (h)	TT_{d2} (h)	ΔTT_s (h)	ΔTT_i (h)	ΔTT_h (h)	ΔTT_{d2} (h)
1	19970209	1249	58.3	66	68.8	74.5	72.5	7.7	10.5	16.2	14.5
2	19970410	1258	71	71.1	73.1	60	50.8	0.1	2.1	−11.0	−20.2
3	19970515	0115	68	45.8	29.5	36.7	46.7	−22.2	−38.5	−31.3	−21.3
4	19971106	2218	64.2	51.9	40	40.9	50.9	−12.3	−24.2	−23.3	−13.3
5	19971130	0714	65.9	86.7	mhd	87.7	74.1	20.7	mhd	21.7	8.2
6	19980128	1555	41.7	69.1	67.1	54.8	42.5	27.4	25.4	13.1	0.9
7	19980523	0100	87.1	69.3	75.8	63.1	45.2	−17.8	−11.3	−24.0	−41.9
8	19980613	1854	56.8	64.5	58.7	68.9	54.1	7.7	1.9	12.1	−2.7
9	19980811	2240	91.4	78.5	82	79.7	72.4	−12.9	−9.4	−11.7	−18.9
10	19980826	0639	32.7	47.1	31.6	37	55.2	14.5	−1.0	4.4	22.5
11	19980906	0815	66	67.7	58.7	71.7	54.1	1.7	−7.3	5.7	−11.8
12	19980924	2320	40.4	43.9	31.7	32.1	39.8	3.5	−8.7	−8.3	−0.6
13	19981002	0705	41.5	63.2	mhd	76.5	11.6	21.6	mhd	34.9	−29.9
14	19981023	1256	61.6	58.5	mhd	81.7	26.9	−3.1	mhd	20.1	−34.7
15	19981108	0420	56.5	63.1	56.8	54.2	23.5	6.6	0.3	−2.3	−32.9
16	19981130	0510	47.3	54.7	48.2	49.1	38.2	7.4	0.9	1.8	−9.0
17	19981226	0952	74.9	56.2	64.2	62	70.8	−18.7	−10.7	−12.9	−4.0
18	19990122	1947	47.7	71.4	mhd	96.9	48.8	23.7	mhd	49.2	1.1
19	19990211	0858	51.7	84.2	mhd	58.7	56.5	32.5	mhd	7	4.8
20	19990218	0208	47.2	55.4	49.3	51	23.5	8.2	2.1	3.8	−23.6
21	19990221	2200	120.6	73	97	111.6	48.1	−47.6	−23.6	−9.0	−72.4
22	19990310	0038	42	74	mhd	94.4	58.1	32	mhd	52.4	16.1
23	19990626	0217	79.9	53	39	42.6	53.7	−26.9	−40.9	−37.3	−26.2
24	19990702	0025	67.2	66	82	59.8	55.1	−1.2	14.8	−7.4	−12.0
25	19990713	0845	56.5	108	mhd	73.8	73.4	51.5	mhd	17.3	16.9
26	19990722	0950	79.6	90	88	66.7	67.8	10.4	8.4	−12.9	−11.8
27	19990728	1338	72	62	mhd	80.4	34.2	−10.0	mhd	8.4	−37.8
28	19990730	1020	40	79	88	37.7	93.8	39	48	−2.3	53.8
29	19990804	0115	52.1	72	72	65.8	60.1	19.9	19.9	13.7	8.1
30	19990808	1745	49.1	73	mhd	45.3	43.5	23.9	mhd	−3.8	−5.5
31	19990823	1130	60.2	69	mhd	114.7	82.1	8.8	mhd	54.5	21.9
32	19990823	1503	46.2	mhd	mhd	65.1	70.8	mhd	mhd	18.9	24.6
33	19990831	0131	55.4	58	72	49.9	57.5	2.6	16.6	−5.5	2
34	19990902	0935	63.5	56	62	63	48.1	−7.5	−1.5	−0.5	−15.4
35	19990915	2005	51.7	62	100	55.6	68.8	10.3	48.3	3.9	17
36	19991119	2224	60.4	69	62	56	38.5	8.6	1.6	−4.4	−21.9
37	19991123	1845	68.1	68	63	51.4	48.1	−0.1	−5.1	−16.7	−20.0
38	19991128	1801	90.5	83	mhd	99.4	67.8	−7.5	mhd	8.9	−22.7
39	19991226	2126	115.4	100	mhd	77	95.8	−15.4	mhd	−38.4	−19.7
40	19991230	1601	63.1	81	mhd	59	53.1	17.9	mhd	−4.1	−9.9
41	20000122	0023	79.1	mhd	mhd	80.7	87.1	mhd	mhd	1.6	8
42	20000211	0213	65.3	61	76	88	74.4	−4.3	10.7	22.7	9.2
43	20000211	2318	45.5	52	40	53.2	49.9	6.5	−5.5	7.7	4.4
44	20000214	0656	50.8	57	78	67.9	72.1	6.2	27.2	17.1	21.3
45	20000220	2050	59.5	61	mhd	67.7	82.6	1.5	mhd	8.2	23.1
46	20000406	1603	48.6	45	45	43.6	53.7	−3.6	−3.6	−5.0	5.1
47	20000424	0851	83.6	mhd	mhd	75.8	76.4	mhd	mhd	−7.8	−7.2
48	20000502	1044	50.7	68	63	43.9	74.1	17.3	12.3	−6.8	23.5
49	20000512	1712	45.6	74	64	62.4	76.4	28.4	18.4	16.8	30.9
50	20000516	1330	86.2	80	102	84.7	82.8	−6.2	15.8	−1.5	−3.5
51	20000523	2315	89.3	75	100	71.1	83.8	−14.3	10.7	−18.2	−5.6
52	20000608	0840	41.3	49	38	36.6	50.9	7.7	−3.3	−4.7	9.6
53	20000611	0716	87.4	57	59	53.2	67.8	−30.4	−28.4	−34.2	−19.6
54	20000618	1702	69.3	52	88	75.2	57.5	−17.3	18.7	5.9	−11.7
55	20000621	1500	85	mhd	mhd	100	63.5	mhd	mhd	15	−21.6
56	20000623	1226	64.9	76	70	51.5	61.5	11.1	5.1	−13.4	−3.4
57	20000710	0558	66.7	69	69	82.8	65.8	2.3	2.3	16.1	−0.9
58	20000713	0918	59.9	46	45	51.6	58.1	−13.9	−14.9	−8.3	−1.8
59	20000714	1532	43.3	65	mhd	84.8	58.5	21.7	mhd	41.5	15.2
60	20000715	1437	28.3	29	25	27.7	34.1	0.7	−3.3	−0.6	5.8
61	20000719	1448	42.5	mhd	mhd	46.7	74.4	mhd	mhd	4.3	32
62	20000725	1322	73.9	64	mhd	70.6	54.2	−10.0	mhd	−3.4	−19.7
63	20000728	0541	74.9	80	68	49.2	63.5	5.1	−6.9	−25.7	−11.3
64	20000906	1612	117.8	mhd	mhd	117.6	78.8	mhd	mhd	−0.2	−39.0
65	20000915	0359	63.9	48	41	56.9	58.2	−15.9	−22.9	−7.0	−5.6
66	20001003	0007	34.9	54	41	43.8	51.9	19.1	6.1	8.9	17
67	20001012	2144	70.1	57	46	56.4	63.5	−13.1	−24.1	−13.7	−6.6
68	20001031	1630	62.7	57	48	55.2	11.6	−5.7	−14.7	−7.5	−51.1
69	20001104	0130	57.3	73.7	73.7	83.8	68.1	16.4	16.4	26.5	10.8
70	20001126	0455	53.5	69.6	54.3	27.6	57.2	16.1	0.8	−25.9	3.8
71	20001128	0500	58.3	60.5	53.7	58.3	62.5	2.2	−4.6	0	4.3
72	20001129	0300	71.9	51.4	72.7	69.9	65.8	−20.5	0.8	−2.0	−6.0

Table 2. (continued)

Event	SAT Date	SAT Time (UT)	TT_o (h)	TT_s (h)	TT_i (h)	TT_h (h)	TT_{d2} (h)	ΔTT_s (h)	ΔTT_i (h)	ΔTT_h (h)	ΔTT_{d2} (h)
73	20001129	0300	58.1	48.7	65.6	56.1	55.2	−9.4	7.5	−2.0	−2.8
74	20001203	0523	94.9	mhd	mhd	115.5	83.8	mhd	mhd	20.6	−11.1
75	20001221	1009	71	85.8	87.6	53.8	73.1	14.8	16.6	−17.2	2.2
76	20010113	0140	73	55.9	49	50.3	38.6	−17.1	−24.0	−22.7	−34.3
77	20010123	1008	60.9	61.9	50.8	40.8	52.8	1	−10.1	−20.1	−8.1
78	20010131	0730	63.5	65.9	mhd	75	49.2	2.4	mhd	11.5	−14.3
79	20010212	2045	43.7	74.9	mhd	mhd	68.4	31.2	mhd	mhd	24.8
80	20010220	0054	107.8	46.7	43.3	58.9	51.2	−61.1	−64.5	−48.9	−56.5
81	20010319	1020	84.3	85.4	84.6	58	78.8	1	0.2	−26.4	−5.6
82	20010322	1242	99.8	mhd	mhd	mhd	85.4	mhd	mhd	mhd	−14.5
83	20010330	2150	57.2	39.3	40.9	mhd	53.2	−17.9	−16.3	mhd	−3.9
84	20010331	0030	38.4	42.1	32.3	mhd	46.7	3.7	−6.1	mhd	8.3
85	20010402	2351	60.3	44.5	49.5	mhd	41.6	−15.8	−10.8	mhd	−18.7
86	20010407	1659	47.6	48.1	53.4	52.6	40.9	0.5	5.8	5	−6.6
87	20010408	1035	39.2	41.2	31.8	26.7	28.6	2	−7.4	−12.5	−10.6
88	20010411	1311	45.7	50.7	51.6	39.6	63.8	5	5.9	−6.1	18.1
89	20010413	0705	41.8	37.8	41	42.7	42.6	−4.0	−0.8	0.9	0.8
90	20010428	0430	38.9	49.4	41.1	48.4	53.2	10.5	2.2	9.5	14.3
91	20010527	1417	66.6	57.4	75.2	81.3	68.4	−9.2	8.6	14.7	1.8
92	20010618	0154	63.8	71.4	64.3	62.9	52.5	7.6	0.5	−0.9	−11.2
93	20010803	0620	81.6	mhd	mhd	mhd	61.1	mhd	mhd	mhd	−20.4
94	20010817	1017	69.6	56.6	60.3	74.3	67.1	−13.0	−9.3	4.7	−2.4
95	20010827	1919	50.8	49.7	37.9	50.5	39.6	−1.1	−12.9	−0.3	−11.1
96	20010830	1326	45.4	59.8	mhd	29.4	38.9	14.4	mhd	−16.0	−6.4
97	20010901	0046	47	73.8	mhd	58.2	55.8	26.8	mhd	11.2	8.9
98	20010901	0108	28.5	56.6	60.3	74.3	47.8	28.1	31.8	45.8	19.2
99	20010914	0119	106	89.5	67.7	62.7	63.8	−16.5	−38.3	−43.3	−42.2
100	20010929	0903	100.4	109.7	109.3	mhd	81.1	9.3	8.9	mhd	−19.3
101	20011011	1620	53.4	64.6	69	68.1	71.4	11.2	15.6	14.7	18
102	20011021	1612	63.2	72.2	57.1	57	58.5	9	−6.1	−6.2	−4.6
103	20011028	0240	59.7	51.3	43.8	52.1	54.2	−8.4	−15.9	−7.6	−5.5
104	20011106	0120	33.2	50.3	35.2	36.8	111.6	17.1	2	3.6	78.5
105	20011109	0403	21	61.2	68.7	50	54.2	40.2	47.7	29	33.2
106	20011119	1735	60.8	68.2	mhd	110.2	73.8	7.4	mhd	49.4	13
107	20011124	0545	64.3	60.8	63.1	67.6	69.1	−3.6	−1.3	3.2	4.8
108	20011124	0800	35.5	66.9	mhd	83.6	52.5	31.4	mhd	48.1	17
109	20011124	0800	33.5	55.3	54.6	52.5	53.2	21.8	21.1	19	19.8
110	20011229	0456	71.9	38.6	42.6	49	57.4	−33.3	−29.3	−22.9	−14.5
111	20011230	1932	47.5	60.6	mhd	84.6	58.4	13.1	mhd	37.1	11
112	20020107	1126	105.1	87.6	107	78.7	92.1	−17.5	1.9	−26.4	−13.0
113	20020126	1535	73.9	83.9	mhd	75.3	88.8	10	mhd	1.4	14.9
114	20020131	2040	104.4	88	mhd	mhd	82.8	−16.4	mhd	mhd	−21.7
115	20020228	0400	85.1	84.7	mhd	66.1	36.8	−0.4	mhd	−19.0	−48.3
116	20020315	1801	66.7	70.6	mhd	114.7	59.2	3.9	mhd	48	−7.5
117	20020318	1233	62.3	83.3	97.9	71.7	85.1	21	35.6	9.4	22.8
118	20020320	1307	58.6	45.6	54.2	55.5	21.2	−13.0	−4.4	−3.1	−37.4
119	20020417	1020	74.6	mhd	mhd	75.3	55.1	mhd	mhd	0.7	−19.5
120	20020419	0810	48	60.6	63.3	61.9	31.8	12.6	15.3	13.9	−16.2
121	20020510	1030	78.6	37.1	25.5	31.1	45.3	−41.5	−53.1	−47.5	−33.3
122	20020518	1919	66.8	80.5	110.9	mhd	94.1	13.6	44	mhd	27.2
123	20020521	2059	108.8	70.3	mhd	mhd	mhd	−38.5	mhd	mhd	mhd
124	20020523	1017	36.8	74.6	84.5	45.5	82.4	37.8	47.7	8.7	45.6
125	20020717	1529	43.3	52.9	34	41.9	−3.4	9.5	−9.4	−1.5	−46.7
126	20020719	0940	50.6	58.3	57.9	46.9	15.2	7.7	7.3	−3.7	−35.3
127	20020719	1442	30.9	62.4	73	48.2	24.5	31.5	42.1	17.3	−6.4
128	20020725	1259	60.5	47.6	56.6	51.5	61.6	−12.9	−3.9	−9.0	1.1
129	20020729	1245	63.5	41.9	37.6	55.8	9.6	−21.6	−25.9	−7.7	−53.9
130	20020801	0425	73.8	70.5	96.9	67.3	59.5	−3.2	23.2	−6.4	−14.3

[a]Shock arrival time (SAT) is given as year, month, day (YYMMDD) and as time in UT of the arrival of the shock at near-Earth spacecraft (such as ACE, Wind, and SOHO). Detailed information about these events can be found in the work of *Fry et al.* [2003] and *McKenna-Lawlor et al.* [2006]. TT_o is the observed transit time. TT_s, TT_i, TT_h, and TT_{d2} are the transit times predicted by STOA, ISPM, HAFv.2, and the Database-II method, respectively. ΔTT_s, ΔTT_i, ΔTT_h, and ΔTT_{d2} are the errors predicted by STOA, ISPM, HAFv.2, and the Database-II method, respectively. The abbreviation mhd indicates that the model predicts that this shock has decayed to an MHD wave before its arrival at L1.

corresponding IP shock arrival at 1 AU are not included here. The list of events includes the year, month, and day of the events; the time of the events' onset; the heliographic latitude and longitude of the events source; the type II speed V_s in km/s; the event duration τ in hours; the associated flare classifications at X-ray and optical wavelengths; and finally, the solar wind speed V_{sw} in km/s at L1 measured at the time of the event.

[33] By applying the Database-I method to the data set of 130 events, we obtained our tentative results on the prediction of the shock arrival times (see Figure 3). The prediction error

Table 3. Comparison of Statistical Results for the Samples Using Different Models, for Hit Windows ±12 h, ±24 h, and ±36 h

Number of Events	Model	Hit (±12 h)	Hit (±24 h)	Hit (±36 h)
130	STOA	58 (45%)	100 (77%)	112 (86%)
130	ISPM	51 (39%)	71 (55%)	81 (62%)
130	HAFv.2	63 (48%)	96 (74%)	106 (82%)
130	Database-II	57 (44%)	101 (78%)	114 (88%)

defined by $\Delta TT_{d1} = TT_{d1} - TT_o$, where TT_o is the observed transit times and TT_{d1} is the predicted transit times by Database-I, respectively. The prediction errors range from −40 h to 100 h, and the result seems unacceptable. In section 4.2, we investigate the dependence of the initial shock speed and longitude on the HAFv.1 computations, and use this to improve the prediction method, creating Database-II.

4.2. Dependencies in HAF Code

[34] In Figure 4a we present shock transit times (*TT*), using the HAF code, from the Sun to the Earth as a function of the sine of (west) heliographic longitude of the initiating source, to demonstrate another way of examining the uncertainty in *TT*. These shocks are subdivided into those with initial speeds 500 km/s, 1000 km/s, and 2000 km/s so that they are individually representative of small, moderately large, and very large events. The longitude ranges from 0° (disk center) to 90° (at the limb). The transit times of shocks located at the heliographic latitude of 0° (solid line), N20° (dotted line), and S20° (dashed line) are shown in Figure 4a. It is seen that the transit time is not particularly sensitive to the latitude of the flare site.

[35] From Figure 4a, it can be seen that the initial speed of the disturbance (V_s) has its greatest effect on the forecast transit time. Flare longitude does not have much of effect on the forecasting result if the event is initiated near disk center. Shocks from flares at the longitude of 0° and at the longitude of 40° are predicted to reach the Earth in about the same amount of time. However, source longitude has an impact on the transit time for large events near the solar limb. The differences in *TT* predicted by using the HAF code for shock events with initial speeds of 1000 km/s and 2000 km/s are about 20 h for shocks at longitudes 60° and 90°, and somewhat less (10 h) for shocks at lower longitudes. These points are also pointed out by *McKenna-Lawlor et al.* [2006].

[36] Figure 4b shows that the transit time decreases with the increase of the initial shock speed for the heliographic longitudes of E20° (dashed line), 0° (black solid line), W20°

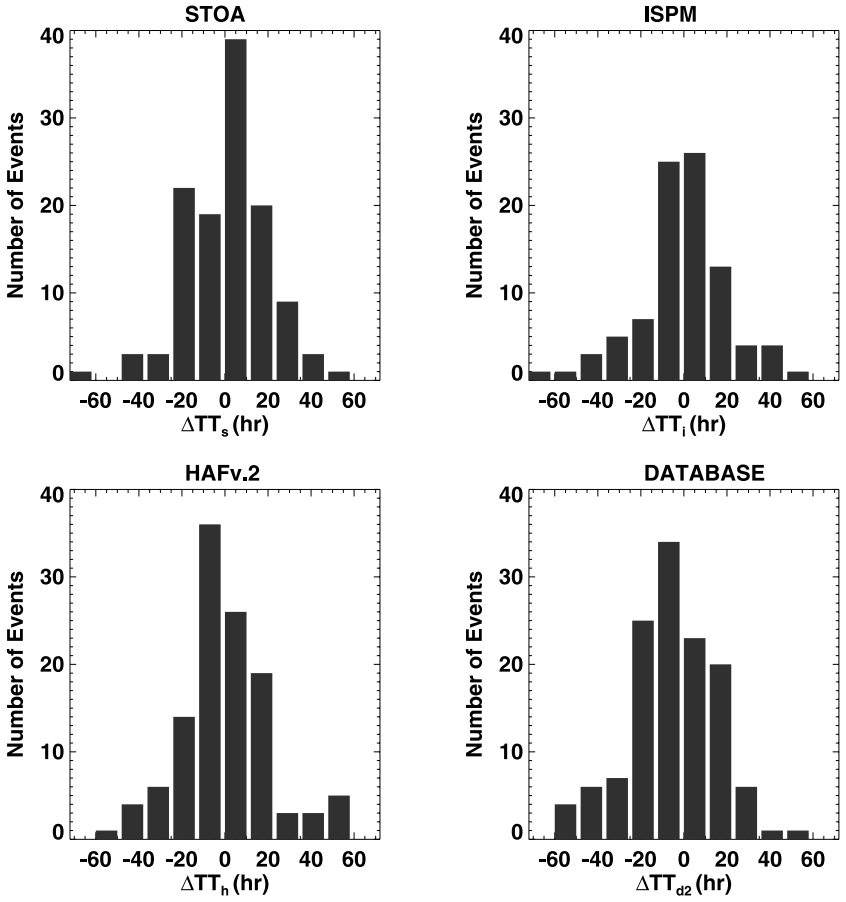

Figure 5. Histograms showing the transit time error (ΔTT_{d2}) between predicted and observed values for the ensemble of models. The transit time error is based on the shock time of arrival (STOA) model, the interplanetary shock propagation model (ISPM), the Hakamada-Akasofu-Fry version 2 (HAFv.2) model, and the Database-II method.

Table 4. Testing the Hypothesis $\Delta TT_{d2} = 0$

Model	ΔTT_{d2} Mean Values (h)	Low Mean Values (h)	Upper Mean Values (h)
STOA	2.803	−12.389	12.633
ISPM	−0.068	−11.287	10.693
HAFv.2	−0.503	−10.790	11.702
Database-II	−2.111	−13.729	13.537

(dotted line), W40° (gray solid line), and W60° (light gray solid line). This also demonstrates that initial shock speed is an important factor contributing to the shock's transit time on its route to 1 AU. The differences in *TT* predicted by the HAF code for shock events with initial shock speed at 200 km/s and 1200 km/s are about 60 h and somewhat less (10 h) for shocks with higher speed.

4.3. Shock Transit Time Database-II

[37] Figure 3a gives the prediction error plotted against the initial shock speed for $V_s \leq 1200$ km/s. The solid line denotes the linear fitting with V_s, ΔTT_{d1} $(V_s) = -7.269 + 0.063V_s$, which can well depict the correlation as seen. Figure 3b gives the prediction error plotted against the heliographic longitude for $V_s > 1200$ km/s. The solid line denotes the linear fitting with the heliographic longitude (φ), ΔTT_{d1} $(\varphi) = 9.544 - 0.328\ \varphi$. The correlations between ΔTT_{d1} and V_s, φ imply that it might be inappropriate to directly use Database-I mentioned above alone. In fact, the initial shock speeds, which were determined using metric radio burst data, have great effect on the shock arrival time (see section 4.2). Also, the input type II speed needs to be adjusted to improve the HAF code's forecasting. This might partially explain why ΔTT_{d1} are correlated with V_s for $V_s \leq$ 1200 km/s. For higher initial shock speed, the transit time is more sensitive to heliograph longitude φ than initial shock speed V_s (see section 4.2). This might partially explain why ΔTT_{d1} are correlated with φ for $V_s > 1200$ km/s. Taking all of these arguments into account, we revise Database-I for predicting the transit time as follows: $TT_{d2} = TT_{d1} + \Delta TT_{d1}$ (V_s), for $V_s \leq 1200$ km/s, and $TT_{d2} = TT_{d1} + \Delta TT_{d1}$ (φ), for $V_s > 1200$ km/s, where TT_{d2} stands for the transit time obtained from the modified database (named Database-II).

[38] For an observed solar transient event, the estimated shock arrival time can be determined by using Database-II. The new prediction results are represented in section 5.

5. Database-II Prediction Results and Comparisons

[39] An extensive set of real-time studies, using HAFv.2 model, has been made during solar cycle 23 for special epochs by *Sun et al.* [2002a, 2002b], *Dryer et al.* [2004], and *McKenna-Lawlor et al.* [2002]. In this section, we discuss the results of our study with the Database-II method mentioned above and comparisons of our results will be made with those of the other three models of STOA, ISPM, and HAFv.2.

Table 5. The 32 Events, Taken From the SOHO Shock List, During the Period September 2002 to July 2005 and the Arrival Times Predicted by our Database-II Method

Event	Begin Date	Begin Time (UT)	Source Location	V_s (km/s)	Arrival Date	Arrival Time	TT_o (h)	TT_{d2} (h)	ΔTT_{d2} (h)
1	20020905	1706	N09°, W28°	679	0907	1554	46.8	54.4	7.6
2	20020915	1738	S05°, W29°	700	0917	2142	52.1	41.1	−10.9
3	20020930	0422	N11°, E10°	1062	1002	2208	65.8	22.2	−43.5
4	20021106	0532	S13°, E13°	405	1109	1756	84.4	93.1	8.7
5	20021222	0252	N23°, W42°	833	1224	1318	58.4	39.8	−18.6
6	20030212	0151	S05°, W43°	700	0214	1739	63.8	47.1	−16.7
7	20030421	1307	N18°, E02°	1223	0424	1819	77.2	22.6	−54.6
8	20030527	2307	S07°, W17°	900	0529	1152	36.8	40.5	3.8
9	20030614	0154	N22°, W15°	875	0616	1800	64.1	43.8	−20.3
10	20030615	2354	S07°, E80°	950	0618	0442	52.8	24.5	−28.3
11	20030617	2255	S07°, E55°	965	0620	0804	57.2	22.5	−34.6
12	20030814	2006	S30°, E00°	378	0817	1345	65.7	66.4	0.7
13	20031022	0956	S02°, E22°	575	1024	1447	52.8	56.8	3.9
14	20031029	2054	S15°, W02°	813	1030	1619	19.4	44.8	25.4
15	20031104	1953	S19°, W83°	1500	1106	1856	47.0	69.2	22.2
16	20031113	0929	N01°, E90°	1100	1115	0527	44.0	11.9	−32.0
17	20031118	0850	S00°, E18°	950	1120	0835	47.8	29.5	−18.2
18	20031120	0747	N01°, W08°	900	1122	0959	50.2	40.5	−9.7
19	20040120	0743	S16°, W12°	965	0122	0110	41.5	67.5	26.1
20	20040406	1328	S18°, E15°	550	0409	0147	60.3	89.8	29.4
21	20040408	1019	S15°, W11°	915	0410	1925	57.1	67.5	10.4
22	20040722	0830	N02°, E08°	899	0724	0532	45.0	72.8	27.8
23	20040725	1514	N08°, W33°	898	0726	2228	31.2	71.8	40.6
24	20040912	0056	N03°, E49°	800	0913	1929	42.5	70.8	28.3
25	20041104	2330	N08°, E18°	1055	1107	0155	50.4	61.2	10.8
26	20041106	0034	N10°, E08°	1000	1107	1759	41.4	61.2	19.8
27	20041107	1654	N09°, W17°	697	1109	0925	40.5	84.4	43.9
28	20041208	1959	N05°, W03°	808	1211	1303	65.1	72.8	7.8
29	20050120	0701	N12°, W58°	882	0121	1648	33.8	89.8	56.1
30	20050513	1657	N12°, E12°	1128	0515	0219	33.4	71.9	38.6
31	20050526	1420	S09°, E14°	586	0529	0915	66.9	108.8	41.8
32	20050714	1120	N11°, W90°	1236	0717	0123	62.0	65.6	3.6

Table 6. Statistical Results for the Samples Listed in Table 5 Using the Database-II Method, for Hit Windows ±12 h, ±24 h, and ±36 h

Number of Events	Model	Hit (±12 h)	Hit (±24 h)	Hit (±36 h)
32	Database-II	10 (31%)	16 (50%)	24 (75%)

[40] The successful prediction should include correctly forecasting shocks (“hits”) and correctly forecasting “no shock” (“correct nulls”). In this paper, the Database-II method is tested only on the basis of events with associated 1 AU shocks. For this purpose, the 130 events, which had been used as a testing set for the HAF model [*Fry et al.*, 2003], are selected. The IP shock observations and prediction results at L1 are listed in Table 2. Table 2 presents the following information: observed shock arrivals, predictions by each model; predicted minus observed SATs. More explicitly, the columns show each event number from Table 1; shock arrival time; the observed transit time TT_o ; the transit time TT_s, TT_i, TT_h, and TT_{d2} predicted by STOA, ISPM, HAFv.2 models and the Database-II method, respectively; and the predicted minus the observed transit times, ΔTT, respectively.

[41] Table 3 shows the success rate within different hit windows for the STOA, ISPM, and HAFv.2 models and the Database-II method. It can be seen that the success rates of the Database-II method is 44% for the hit window of ±12 h, 78% for window of ±24 h, and 88% for window of ±36 h. As shown in Table 3, the performances of the four models within the same hit window are nearly identical as well.

[42] We may now test the hypothesis whether the theoretical ΔTT (i.e.,ΔTT_s, ΔTT_i, ΔTT_h, and ΔTT_{d2}) is zero for each of the models. As shown in Figure 5, the distribution of ΔTT is approximately Gaussian with a peak around zero. The mean values of prediction errors would be around zero for the four models. On the basis of hit data, the confidence levels (hit window = ±36 h) were calculated separately for positive and negative ΔTT for the sample events (see Table 4).

[43] In order to test the Database-II method, we choose 32 events with associated shocks at 1 AU (listed in Table 5) during the period from September 2002 to July 2005, from the SOHO shock list (available at http://umtof.umd.edu/pm/FIGS.HTML), as a new testing set. The statistical results of the Database-II method predictions are presented in Table 6. The success rate of the Database-II method is 31% for the hit window of ±12 h; 50% for the hit window of ±24 h; 75% for the hit window of ±36 h. It can be seen that this set does worse than initial data set. This may be due to the fact that this time period contained active periods during which there were large variations of the magnetic field on solar surface.

[44] An additional collection of 23 events from *Smith and Dryer* [1995] (listed in Tables 7 and 8) during the period from January 1979 to October 1989 is utilized to validate the applicability to other cycles. For these events, the year of occurrence of the event is taken to be the corresponding year in the 23rd solar cycle, related by phase in solar activity. Table 9 shows the success rates within different hit windows for the STOA model, the ISPM model, and the Database-II method during this period. It can be seen that the success rate of the Database-II method is 35% when the hit window is ±12 h; 57% for window of ±24 h; 70% for window of ±36 h. Here, the results in Database-II established for cycle 23 are used for events that occurred in other solar cycles, and this may probably be the reason that the results for this set is worse than for the initial. As shown in Table 9, the Database-II method seems to perform well for the previous solar cycle. Thus, this Database-II method may possibly be applicable to other cycles.

6. Conclusions

[45] A practical database (i.e., Database-II) method for predicting the arrival time of IP shocks at Earth is introduced.

Table 7. Input Parameters of the 23 Events, Taken From *Smith and Dryer* [1995], During the Period January 1979 to October 1989

Event	Begin Date	Begin Time (UT)	Source Location	V_s (km/s)	τ (h)	Flare Classification: X-ray/Optical	V_{sw} (km/s)
1	19790103	2148	S12°, W02°	1400	0.10	M1.0/?B	412
2	19790216	0149	N16°, E59°	1222	0.90	X2.0/3B	390
3	19790502	1700	N20°, W55°	1100	0.45	X1.0/2B	360
4	19790704	1920	N21°, E36°	1444	1.80	M1.0/1B	308
5	19791106	0516	N19°, E11°	1350	1.10	X1.0/1N	373
6	19791108	0118	N31°, E73°	1380	0.58	M5.0/1B	420
7	19791219	2212	S15°, E36°	1500	0.42	X1.0/2B	370
8	19800409	2237	S10°, W90°	1500	1.37	C7.0/2B	424
9	19800521	2057	S14°, W15°	1068	0.77	X1.0/3B	400
10	19800603	2133	S14°, E65°	1600	0.55	M7.0/2B	301
11	19800822	0533	N09°, E58°	1300	0.12	M1.0/1B	385
12	19810215	1901	N15°, W71°	795	0.35	M1.0/1B	377
13	19810226	1953	S14°, E49°	1200	0.25	X4.0/3B	338
14	19810404	0508	S44°, W88°	1000	0.03	X1.0/2B	400
15	19810410	1110	N11°, E53°	1807	0.62	X1.0/1B	419
16	19810424	1355	N18°, W50°	1970	1.42	X6.0/2B	500
17	19810513	0405	N11°, E55°	1500	2.00	X2.0/3B	500
18	19810516	0824	N14°, E14°	1750	2.00	X1.0/3B	450
19	19810828	0347	N10°, W44°	1678	0.12	M6.0/1B	337
20	19820603	1144	S09°, E72°	1000	0.38	X8.0/2B	652
21	19820606	1634	S09°, E25°	1250	1.25	X9.0/3B	650
22	19820618	2146	N19°, W11°	1000	0.40	M1.0/1B	448
23	19820619	1958	N14°, W24°	600	0.25	M2.0/2B	331

Table 8. Observed and Predicted Arrival Times for the 23 Events in Table 7

Event	SAT Date	SAT Time (UT)	TT_o (h)	TT_s (h)	TT_i (h)	TT_{d2} (h)	ΔTT_s (h)	ΔTT_i (h)	ΔTT_{d2} (h)
1	19790106	0127	51.7	62.8	49.0	41.5	11.1	−2.7	−10.2
2	19790218	2027	66.6	68.0	68.8	34.6	1.4	2.2	−32.0
3	19790505	0850	63.8	81.9	mhd	43.9	18.1	mhd	−19.9
4	19790706	1930	48.2	49.4	37.9	50.0	1.2	−10.3	1.8
5	19791107	1349	32.5	60.3	38.0	98.2	27.8	5.5	65.6
6	19791111	0225	73.1	65.3	mhd	66.9	−7.8	mhd	−6.2
7	19791222	0500	54.8	49.4	47.3	44.0	−5.4	−7.5	−10.8
8	19800411	1500	40.4	62.6	mhd	92.9	22.2	mhd	52.5
9	19800524	0700	58.0	69.3	53.8	11.2	11.3	−4.3	−46.8
10	19800606	1100	61.5	78.3	62.4	60.2	16.9	1.0	−1.2
11	19800825	2300	89.4	69.8	mhd	68.8	−19.6	mhd	−20.6
12	19810219	1900	96.0	84.4	mhd	29.1	−11.6	mhd	−66.8
13	19810301	0738	59.8	82.3	74.8	−2.4	22.6	15.1	−62.1
14	19810407	1954	86.8	mhd	mhd	9.2	mhd	mhd	−77.5
15	19810412	1419	51.2	52.1	45.9	29.5	0.9	−5.3	−21.7
16	19810426	1339	47.7	32.4	18.7	43.8	−15.3	−29.0	−3.9
17	19810514	0813	28.1	47.2	35.0	34.5	19.1	6.9	6.4
18	19810517	1857	34.5	44.7	44.3	31.6	10.2	9.8	−3.0
19	19810830	2300	67.2	38.8	26.3	46.2	−28.4	−40.9	−21.1
20	19820606	1631	76.8	54.7	mhd	58.2	−22.1	mhd	−18.5
21	19820609	0040	56.1	48.1	43.0	49.6	−8.0	−13.1	−6.5
22	19820622	1336	87.8	65.2	62.5	61.2	−22.6	−25.3	−26.6
23	19820624	1900	119.0	96.4	121.9	84.4	−22.6	2.9	−34.6

Database-II for shock transit time is established by computing the transit times using the HAF code from the following input data: the source location, initial shock speed and the year of occurrence within a solar cycle of an observed solar transient event. Database-II consists of this information stored in a mesh. Thus the arrival time at L1 for any given solar event occurring in solar cycle 23 can be obtained by comparing the mesh grid/hypothetical event of Database-II and that of the solar event.

[46] Applying the Database-II method to 130 solar events during the period from February 1997 to August 2002, we found that the performance of our model is as good as those of the STOA, ISPM, and HAFv.2 models in predicting the shock arrival time. Our Database-II method promptly provides arrival times, from three parameters obtained from solar observations. An additional 32 solar events during the periods from September 2002 to July 2005 are utilized to test the Database-II method as a new testing set and good performance is presented. These results demonstrate the feasibility of our model as one of the shock arrival time prediction methods in real-time space weather forecasting.

[47] To check the applicability of the long-term periodicity in solar activity, we tested the Database-II method on a new set of events during the period from January 1979 to October 1989. Its performance compares well to those of the STOA and ISPM models. That is, this Database-II method may possibly be applicable to other solar cycles.

Table 9. Comparison of Statistical Results for the Samples Listed in Tables 7 and 8 Using Different Models, for Hit Windows ±12 h, ±24 h, and ±36 h

Number of Events	Model	Hit (±12 h)	Hit (±24 h)	Hit (±36 h)
23	STOA	10 (43%)	20 (87%)	22 (96%)
23	ISPM	11 (48%)	13 (57%)	15 (65%)
23	Database-II	8 (35%)	13 (57%)	16 (70%)

[48] There are two improvements for future consideration. On one hand, the shock arrival time of a solar event can be changed with the variation of background conditions. However, the Database-II method does not utilize the real-time magnetic field on the solar source surface, which provides the steady magnetic field boundary conditions that drive the HAF model background solar wind. Instead, it uses the mean magnetic field of all Carrington Rotations in the corresponding year. The prediction error caused by this aspect should be improved in the future study. On the other hand, the database is constructed by using hypothetical shock events with speeds between 200 km/s and 2000 km/s, covering the 23rd solar cycle (excluding shock events with speeds >2000 km/s). The arrival times of the ''average'' observed shock events (shocks with speeds in 200 km/s $\sim$ 2000 km/s) in the 23rd solar cycle can be obtained by our database method. Two concerns are mentioned. On one hand, there are a few shock events with speeds >2000 km/s; on the other hand, shock events with speeds in 2000 km/s $\sim$ 3000 km/s can be easily considered if we add more grids $21 \times 72 \times 10 \times 11$ to our database. In our future work, shock events with speeds in 2000 km/s $\sim$ 3000 km/s will be included in the database. There is a gap in the present database, namely that large shock events with speeds >2000 km/s are not included. But, this is not an essential difficulty, as the method can be modified to include the high-speed intervals.

[49] **Acknowledgments.** We acknowledge Jih-Kwin Chao and C. B. Wang for supplying the HAFv.1 code. We are grateful to the SOHO team for the interplanetary shock list. The authors appreciate and thank the referees for their constructive comments and suggestions. This work is jointly supported by the National Natural Science Foundation of China (40536029, 40621003, and 40523006), 973 Program under grant 2006CB806304, the Specialized Research Fund for State Key Laboratories, and the Special Fund for Public Welfare Industry (meteorology) under contract GYHY200806024.

[50] Zuyin Pu thanks Zdenka Smith and another reviewer for their assistance in evaluating this paper.

References

Arge, C. N., and V. J. Pizzo (2000), Improvement in the prediction of solar wind conditions using near-real-time solar magnetic field updates, *J. Geophys. Res.*, *105*, 10,465–10,479, doi:10.1029/1999JA000262.

Dryer, M., and D. F. Smart (1984), Dynamical models of coronal transients and interplanetary disturbances, *Adv. Space Res.*, *4*(7), 291–301, doi:10.1016/0273-1177(84)90200-X.

Dryer, M., Z. Smith, C. D. Fry, W. Sun, C. S. Deehr, and S.-I. Akasofu (2004), Real-time shock arrival predictions during the "Halloween 2003 epoch", *Space Weather*, *2*, S09001, doi:10.1029/2004SW000087.

Feng, X. S., and X. H. Zhao (2006), A new prediction method for the arrival time of interplanetary shocks, *Sol. Phys.*, *238*, 167–186, doi:10.1007/s11207-006-0185-3.

Fry, C. D. (1985), Three-dimensional structure of the heliosphere: Quiet-time and disturbed periods, Ph.D. thesis, Alaska Univ, Fairbanks.

Fry, C. D., W. Sun, C. S. Deehr, M. Dryer, Z. Smith, S.-I. Akasofu, M. Tokumaru, and M. Kojima (2001), Improvements to the HAF solar wind model for space weather predictions, *J. Geophys. Res.*, *106*, 20,985–21,002, doi:10.1029/2000JA000220.

Fry, C. D., M. Dryer, Z. Smith, W. Sun, C. S. Deehr, and S.-I. Akasofu (2003), Forecasting solar wind structures and shock arrival times using an ensemble of models, *J. Geophys. Res.*, *108*(A2), 1070, doi:10.1029/2002JA009474.

Hakamada, K., and S.-I. Akasofu (1982), Simulation of three-dimensional solar wind disturbance and resulting geomagnetic storms, *Space Sci. Rev.*, *31*, 3–70, doi:10.1007/BF00349000.

Howard, T. A., C. D. Fry, J. C. Johnston, and D. F. Webb (2007), On the evolution of coronal mass ejections in the interplanetary medium, *Astrophys. J.*, *667*(1), 610–625, doi:10.1086/519758.

Lewis, D., and M. Dryer (1987), Shock-Time-of-Arrival Model (STOA-87), contract report (systems documentation) to U.S. Air Force Air Weather Service, NOAA Space Environ. Lab., Boulder, Colo.

Manoharan, P. K., N. Gopalswamy, S. Yashiro, A. Lara, G. Michalek, and R. A. Howard (2004), Influence of coronal mass ejection interaction on propagation of interplanetary shocks, *J. Geophys. Res.*, *109*, A06109, doi:10.1029/2003JA010300.

McKenna-Lawlor, S. M. P., M. Dryer, Z. Smith, K. Kecskemety, C. D. Fry, W. Sun, C. S. Deehr, D. Berdichevsky, K. Kudela, and G. Zastenker (2002), Arrival times of Flare/HALO CME associated shocks at the Earth: Comparison of the predictions of three numerical models with these observations, *Ann. Geophys.*, *20*, 917–935.

McKenna-Lawlor, S., M. Dryer, M. D. Kartalev, Z. Smith, C. D. Fry, W. Sun, C. S. Deehr, K. Kecskemety, and K. Kudela (2006), Near real-time predictions of the arrival at the Earth of flare-generated shocks during Solar Cycle 23, *J. Geophys. Res.*, *111*, A11103, doi:10.1029/2005JA011162.

Moon, Y.-J., M. Dryer, Z. Smith, Y. D. Park, and K. S. Cho (2002), A revised shock time of arrival (STOA) model for interplanetary shock propagation: STOA-2, *Geophys. Res. Lett.*, *29*(10), 1390, doi:10.1029/2002GL014865.

Schwenn, R., A. Dal Lago, E. Huttunen, and W. D. Gonzalez (2005), The association of coronal mass ejections with their effects near the Earth, *Ann. Geophys.*, *23*, 1033–1059.

Smart, D. F., and M. A. Shea (1985), A simplified model for timing the arrival of solar-flare-initiated shocks, *J. Geophys. Res.*, *90*, 183–190, doi:10.1029/JA090iA01p00183.

Smart, D. F., M. A. Shea, W. R. Barron, and M. Dryer (1984), A simplified technique for estimating the arrival time of solar flare-initiated shocks, in *Proceedings of STIP Workshop on Solar/Interplanetary Intervals*, edited by M. A. Shea, D. F. Smart, and S. McKenna-Lawlor, pp. 139–156, Book Crafters, Inc., Chelsea, Mich.

Smart, D. F., M. A. Shea, M. Dryer, A. Quintana, L. C. Gentile, and A. A. Bathurst (1986), Estimating the arrival time of solar flare-initiated shocks by considering them to be blast waves riding over the solar wind, in *Proceedings of the Symposium on Solar-Terrestrial Predictions*, edited by P. Simon, G. R. Heckman, and M. A. Shea, pp. 471–481, U.S. Gov. Print. Off., Washington, D.C.

Smith, Z., and M. Dryer (1990), MHD study of temporal and spatial evolution of simulated interplanetary shocks in the ecliptic plane within 1 AU, *Sol. Phys.*, *129*, 387–405, doi:10.1007/BF00159049.

Smith, Z. K., and M. Dryer (1995), The Interplanetary Shock Propagatio n Model: A model for predicting solar-flare-caused geomagnetic sudden impulses based on the 2-1/2D MHD numerical simulation results from the Interplanetary Global Model (2DIGM), *NOAA Tech. Memo., ERL/SEL-89*.

Smith, Z. K., M. Dryer, E. Ort, and W. Murtagh (2000), Performance of interplanetary shock prediction models: STOA and ISPM, *J. Atmos. Sol. Terr. Phys.*, *62*, 1265–1274, doi:10.1016/S1364-6826(00)00082-1.

Smith, Z. K., T. R. Detman, M. Dryer, C. D. Fry, C. C. Wu, W. Sun, and C. S. Deehr (2004), A verification method for space weather forecasting models using solar data to predict arrivals of interplanetary shocks at Earth, *IEEE Trans. Plasma Sci.*, *32*, 1498–1503, doi:10.1109/TPS.2004.832509.

Sun, W., S.-I. Akasofu, Z. K. Smith, and M. Dryer (1985), Calibration of the kinematic method of studying solar wind disturbances on the basis of a one-dimensional MHD solution and a simulation study of the heliosphere disturbances between 22 November and 6 December 1977, *Planet. Space Sci.*, *33*, 933–943, doi:10.1016/0032-0633(85)90107-2.

Sun, W., M. Dryer, C. D. Fry, C. S. Deehr, Z. Smith, S.-I. Akasofu, M. D. Kartalev, and K. G. Grigorov (2002a), Evaluation of solar type II radio burst estimates of initial solar wind shock speed using a kinematic model of the solar wind on the April 2001 solar event swarm, *Geophys. Res. Lett.*, *29*(8), 1171, doi:10.1029/2001GL013659.

Sun, W., M. Dryer, C. D. Fry, C. S. Deehr, Z. Smith, S.-I. Akasofu, M. D. Kartalev, and K. G. Grigorov (2002b), Real-time forecasting of ICME shock arrivals at L1 during the "April Fools Day" epoch: 28 March–21 April 2001, *Ann. Geophys.*, *20*, 937–945.

Wang, Y. M., and N. R. Sheeley Jr. (1990), Solar wind speed and coronal flux-tube expansion, *Astrophys. J.*, *355*, 726–732, doi:10.1086/168805.

Wang, Y. M., N. R. Sheeley Jr., J. L. Phillips, and B. E. Goldstein (1997), Solar wind stream interactions and the wind speed-expansion factor relationship, *Astrophys. J.*, *488*, L51–L54, doi:10.1086/310918.

Zhao, X. H., X. S. Feng, and C. C. Wu (2006), Characteristics of solar flares associated with interplanetary shock or nonshock events at Earth, *J. Geophys. Res.*, *111*, A09103, doi:10.1029/2006JA011784.

C. S. Deehr and W. Sun, Geophysical Institute, University of Alaska Fairbanks, Fairbanks, AK 99775, USA. (cdeehr@gi.alaska.edu; wsun_1939@yahoo.com)

M. Dryer, Space Weather Prediction Center, National Oceanic and Atmospheric Administration, 325 Broadway, Boulder, CO 80305, USA. (Murray.Dryer@noaa.gov)

X. S. Feng and Y. Zhang, SIGMA Weather Group, State Key Laboratory of Space Weather, Center for Space Science and Applied Research, Chinese Academy of Sciences, P.O. Box 8701, Beijing 100190, China. (fengx@spaceweather.ac.cn; yzhang@spaceweather.ac.cn)

C. D. Fry, Exploration Physics International, Inc., Huntsville, AL 35806, USA. (gfry@expi.com)